We are IntechOpen, the world's leading publisher of Open Access books Built by scientists, for scientists

6,900
Open access books available

185,000
International authors and editors

200M
Downloads

Our authors are among the

154
Countries delivered to

TOP 1%
most cited scientists

12.2%
Contributors from top 500 universities



WEB OF SCIENCE™

Selection of our books indexed in the Book Citation Index in Web of Science™ Core Collection (BKCI)

Interested in publishing with us?
Contact book.department@intechopen.com

Numbers displayed above are based on latest data collected.
For more information visit www.intechopen.com



6

Sintering Characteristics of Injection Moulded 316L Component Using Palm-Based Biopolymer Binder

Mohd Afian Omar and Istikamah Subuki
AMREC, SIRIM Berhad, Lot 34, Jalan Hi Tech 2/3,
Kulim Hi Tech Park, Kulim, Kedah
Malaysia

1. Introduction

Metal injection moulding (MIM) has been widely recognised as an advanced technology for the fabrication of complex-shaped, low cost and high performance components. Fine powders, less than 20 micron in diameter, are mixed with suitable thermoplastic binder and formed into the desired shapes. The binder aids the flowability and formability of fine metal powders during moulding, and they have to be removed in the next stage to enable high density components to be produced. The removal of the binder is done either thermally in the furnace or by solvent extraction. Ideally, the removal of the binder would open up pore channels which allow accelerated removal of the higher boiling point components. The components are sintered following the debinding stage. This stage is crucial to the MIM process as appropriate sintering conditions would ensure pore-free structures that have good mechanical properties (German, 1990; German and Bose, 1997)

Theoretical studies of sintering treat the powder as a spherical particle and divide sintering into three stages. The early stage of sintering occurs at low temperatures and is characterised by neck growth at the contact points between the particles. The intermediate stage of sintering is characterised by an interconnected pore system having complex geometry. (German, 1996)

The final stage begins when the pore phase becomes closed and the shrinkage rate of the components slow down. This final stage characterised by pores on four-grain corners that shrink rapidly, and sphereodised powders that separate from grain boundaries and shrink slowly. When all pores on four-grain corners have been eliminated, sintering densification essentially ceases (German, 1990 ; German 1992, German and Hens, 1993; German, 1996)

There has been a considerable motivation to design and develop binders that are locally produced in order to minimize the manufacturing cost and to fulfill the requirements of the MIM process. Prior study by Johnson (1988) revealed that moulded specimens made with peanut and vegetable oil mixed with polymer binder of polyethylene (PE) and polypropylene (PP), substantially eliminate cracking phenomenon that is commonly observed in the moulding process. These peanut and vegetable oil were used to replace the function of wax and surfactant in a binder system to ensure good wetting of the powder. As the characteristics

of palm oil are similar to those oils mentioned, which consists of glycerides used as a surface active agent in many binder systems, palm oil can be considered as a potential binder. Since Malaysia is one of the largest producers and exporter of palm oil, it can be an opportunity to design a new locally sourced binder system to achieve these goals.

Besides the suitable constituent, palm oil also has other attributes as a binder such as low viscosity, high decomposition temperature, lower molecular weight to avoid residual stress and distortion, environmentally acceptable, inexpensive and easily dissolved in organic solvent. Thus, Iriany (2002) investigated the possibility of palm oil as a binder via characterisation of feedstock. The results indicate that palm oil can be used as a binder component and was found to be compatible with polyethylene and stainless steel powder. However, the investigation was limited to the flow behaviour of the proposed system. To accomplish the investigations through all process of MIM, the new developed binder, palm stearin and feedstock prepared with different particle size, powder loading and binder formulation were studied by considering a variety of aspects. These aspects include torque evaluation curves, rheological behaviour, injection moulding, kinetic solvent extraction, thermal pyrolysis and effect of sintering when specimen is sintered at different temperature, atmosphere, soaking time and heating rate. The results on moulding behavior, rheological behavior and debinding study has been discussed elsewhere. (Omar, 2007; Omar, 2006a and 2006b; Omar 2001; Omar, 2002) However, in this chapter, the results reported was on sintering characteristics of 316L stainless steel powder using palm stearin (PS) as a major portion and a minor fraction of poly propylene (PP).

2. Method and materials

The 90 %-22 μm 316L stainless steel powder used in the present study was obtained from Sandvik. The mean particle size distribution was determined using HELOS Particle Size Analysis WINDOX 5 and around 9 micron A scanning electron micrograph showing the powder morphology is spherical. The powder was mixed with a natural polymer based binder (palm stearin) at a solid loading of 65-volume % for injection molding. The binder system consists of different percentage of palm stearin (PS) and polypropylene (PP), as tabulated in table 1. The mixing was carried out in a sigma blade mixer for 1 hour at 160 ^{o}C to produce feedstock. (Omar, 2007; Omar 2006) The mixing was left for 1 ½ hour. After mixing has completed, the heater was shut off and the feedstock was allowed to cool with the mixing blade still in motion. This procedure gives a granulated feedstock.

Label	Vol.% fraction	Composition, wt.%	
		PS	PP
PSPP65-2	65	50	50
PSPP65-3	65	60	40
PSPP65-4	65	70	30

Table 1. Feedstock made with different composition binder of PS/PP.

The granulated feedstock was then injected into tensile bars using a simple, vertically aligned and pneumatically operated plunger machine, MCP HEK-GMBH. Feedstock was

fed into the barrel and then injected through the nozzle in the mold cavity. Test bars were successfully molded at temperature of 220^{o}C at pressure 300 bar. The dimensions and weight including density were measured in order to determine the solvent removal and shrinkage after sintering. The densities of the specimens were measured using water immersion method.

The test bars were debound by a two-step process where at the first stage the samples were solvent debound in order to remove all the wax portion of the binder, in this case palm stearin which is consist the major fraction of the binder. Molded samples termed the green body were arranged in a glass container, which then immersed in heptane and held at temperature 60^{o}C for 5 hours. The glass container was covered to prevent evaporation of the heptane during extraction Subsequent thermal pyrolysis was performed in Lynn Furnace. The thermal debinding cycle consisted of 3^{o}C/min to 450^{o}C and soaking for 1 hour before furnace cool. Sample that completely undergoes thermal debinding termed the brown body.

The components were sintered in vacuum furnace with the heating rate at 10^{o}C/min to the sintering temperature 1360^{o}C, and held for 1 hour at this temperature before cooled down by furnace cool. The dimensions, density and weight of the sintered specimens were measured to calculate sintered shrinkage and final density.Tensile properties of the sintered samples were determined using an Instron Series IX Automated Materials Testing System. The yield strength, ultimate strength and elongation were measured at strain rate of 0.1/s . Finally, the microstructure analysis was carried out using optical microscopy and scanning electron microscopy.

3. Results and discussion

3.1 Properties of sintered specimen made with various composition of PS/PP

Three different specimens made with different compositions of binder system and labelled as PSPP65-2, PSPP65-3 and PSPP65-4, were sintered at various temperatures. The specimens were sintered under vacuum conditions. The samples were heated to 450^{o}C, soaked for 1 hour with the heating rate 3^{o}C/min and then heated up at a rate of 10^{o}C/min to sintering temperature of 1300^{o}C, 1320^{o}C, 1340^{o}C and 1360^{o}C with a soaking time of 1 hour.

3.1.1 Physical properties

Figure 1 shows the density of the sintered specimens made with PS/PP binder with various compositions as a function of sintering temperature. As the sintering temperature was increased from 1300 ^{o}C to 1360 ^{o}C, the density was improved for all specimens. An increase of 20 ^{o}C of the sintering temperature can improve the sintered density by up to 3%.

It clearly shows that an increase of 10 wt.% of PS resulted in 0.41% to 1.83% improvement in sintered density. The sample PSPP65-4 gave the highest density at all sintering temperatures compared to the other two compositions. It explains that higher PS content can provide better sintered specimen integrity. Table 2 gives the relative density for the samples. It clearly shows that the density data where higher than those of PS/PE (Istikamah, 2010) This circumstance might be due to a higher residual carbon of PS/PP compared to PS/PE system leaving the sample prior to sintering process. This residual carbon which left after debinding, diffused into the structure of SS 316L powder during sintering and eventually increased the density of the sintered specimens.

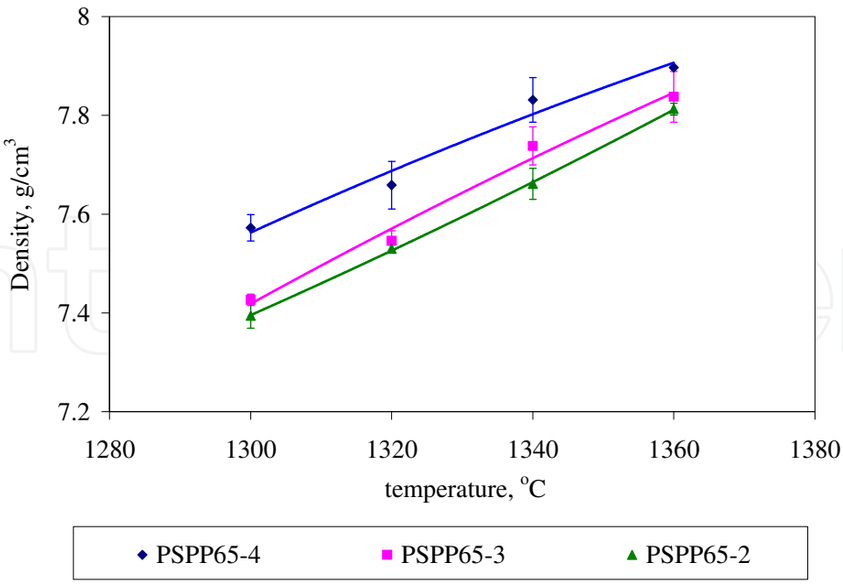


Fig. 1. Effect of PS content on the density of specimen sintered at different temperatures.

sintered specimen	Sintering temperature (°C)			
	1300	1320	1340	1360
PSPP65-2	± 93	± 95	± 96	± 98
PSPP65-3	± 93	± 95	± 97	± 99
PSPP65-4	± 95	± 96	± 98	± 99

Table 2. Relative density (%) of 316L sintered specimens at different wt% of PS/PP and sintering temperature.

Specimen shrinkage as a function of PS/PP contents and sintering temperature is shown in Figure 2. It clearly shows from the study that as the sintering temperature was increased from 1300 °C to 1360 °C there was a progressive increase in shrinkage percentage for all sintered specimens. The same relation was found in the density as discussed before. It shows that greater density results in a greater shrinkage. As the sintering temperature increased, it reduces the pore volume, leading to compact densification and thus increases the sintered density. Simultaneously, more active bulk transport that create a change in the interparticle spacing as neck growth, takes place and as a result increases the linear shrinkage.

This plot gives the highest sintering shrinkage of 15% resulted in 98% final density (Figure 2). The shrinkage is much higher for the specimen made with high content of PS. This may be due to the high shrinkage of brown body during thermal debinding of PP after high composition of PS was totally removed through solvent extraction. Sintering inherently involves substantial shrinkage, the process being characterized by a linear shrinkage of between 10 to 30%. From the result obtained, all specimen show linear contraction and produce good specimen without distortion.

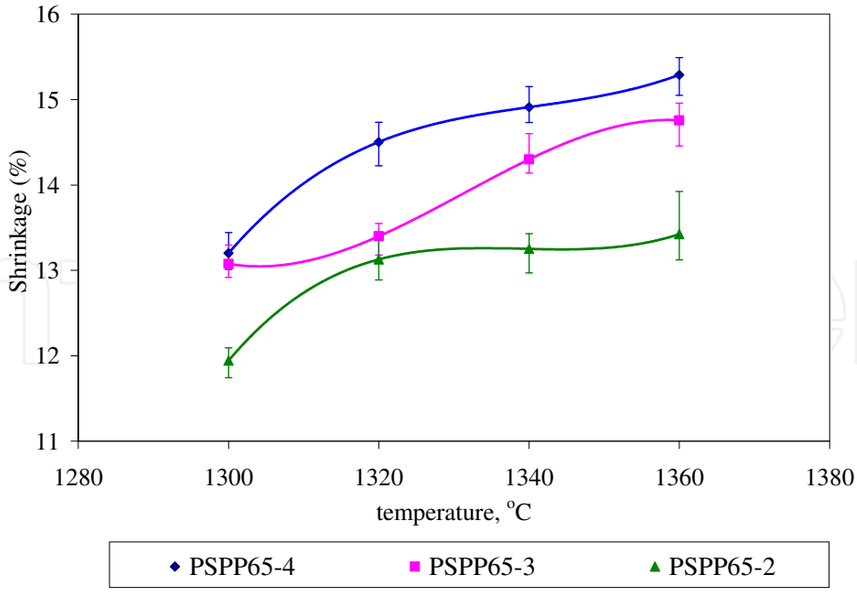


Fig. 2. Effect of sintering temperature on linear shrinkage of specimen made with different composition binder system.

Figure 3 shows the corresponding porosity for all compositions at various temperatures. It clearly shows that the porosity of the sintered specimens decreased as the sintering temperature increased for all specimen tested. Moreover, sintering temperature greater than 1320 °C gives much less deviation as compared to 1300 °C. These might be due to the changes and transformation it undergoes from intermediate to final stage of sintering to become dense and high strength, with attendant changes in the pore size and shape. At lower sintering temperature, there is insufficient fusion of metal powder in order to weld together (German, 1996). As a result, pore volume cannot be reduced as there is an insufficient kinetic energy. However, at higher temperatures especially beyond 1320 °C, this kinetic energy seems to be sufficient to remove free surface with the secondary elimination of grain boundary area via grain growth. (German, 1996)

At this final stage of sintering (1320 °C to 1360 °C), the elimination of isolated spherical pores was difficult, since vacancies must diffuse to distant grain boundaries, which is a very slow process. Also, with prolonged sintering, pore coarsening causes the mean pore size to increase while the number of pores decreases. As a consequence, there are slightly different porosity percentages at this stage of sintering. (Zhang and German, 1991)

Figures 4 to 6 show the optical micrograph of samples sintered at temperatures from 1300 °C to 1360 °C after etching. There is not much difference in grain size observed as temperature is increased. At that temperature, sintering is likely to slow down, as during this final stage of sintering, spherical pores shrink by a diffusion mechanism. The events lead to the isolation of a pore and spheroidisation due to rapid grain growth (German, 1996). At 1360 °C, it shows a change in the grain size as well as a decline in the total porosity during sintering as discussed before. The grain growth increased from 1300 °C to 1360 °C due to the annihilation of the pores on the grain boundaries.

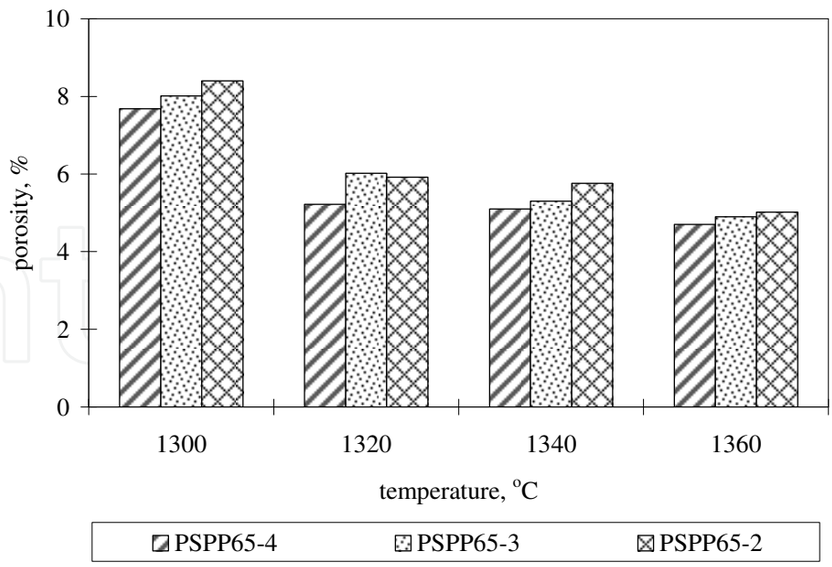
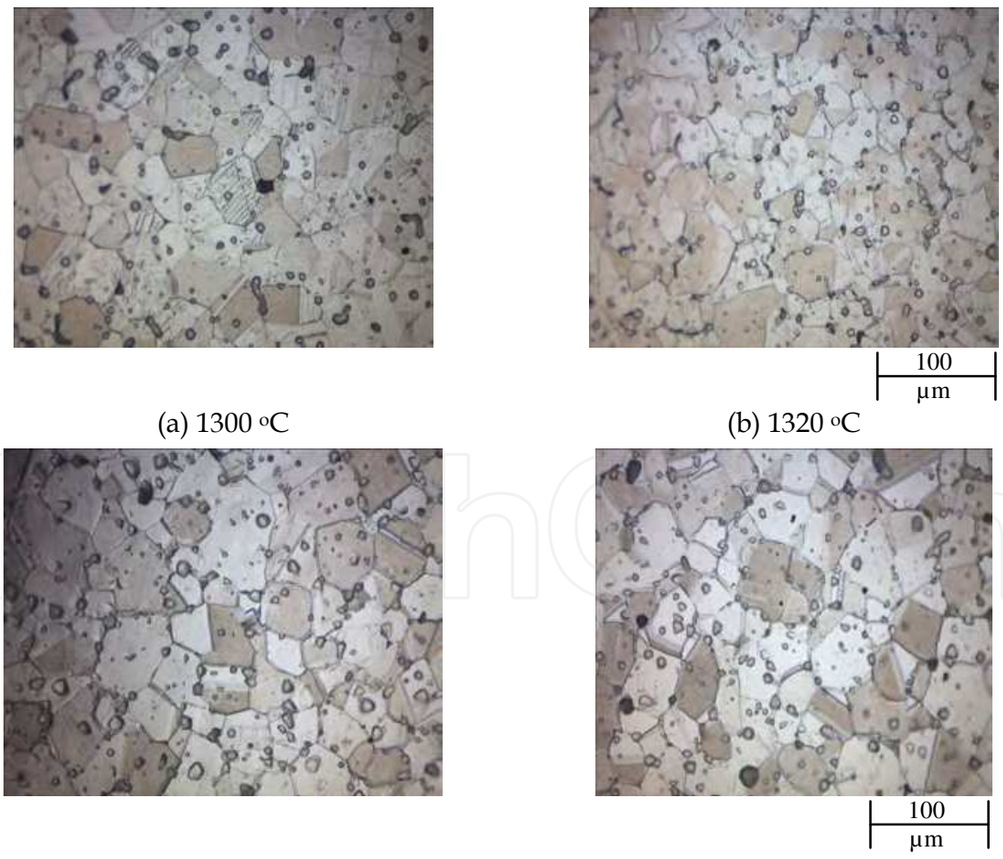


Fig. 3. The porosity of specimen sintered at different temperatures.

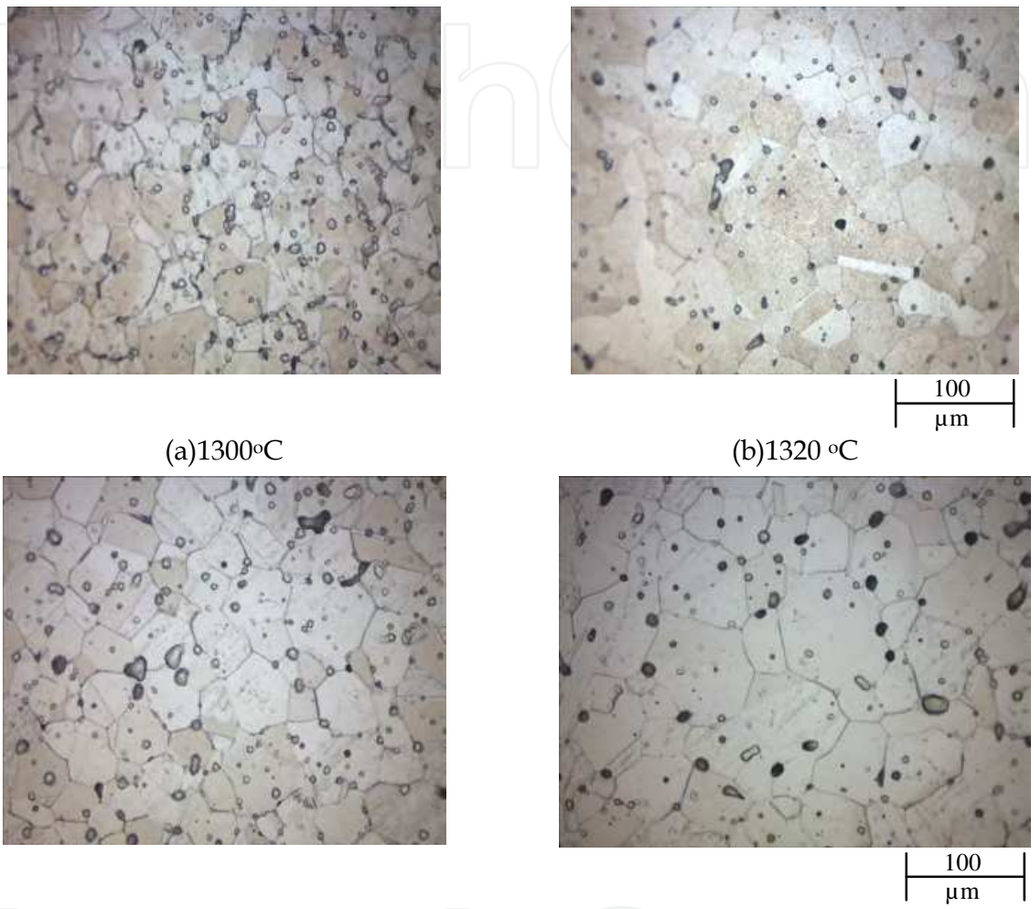


(a) 1300 °C (b) 1320 °C

(c) 1340 °C (d) 1360 °C

Fig. 4. Optical micrographs of PSPP65-4 specimen sintered at various temperatures. Magnification 500x.

As shown in the figure, the pore geometry is highly convoluted and the pores are located at grain boundary intersection. The microstructures show a progression from irregular pores along the particle boundaries a shown in Figure 4. (a), 5 (a) and 6 (a) to spherical pores as shown in Figure 4 (d), 5 (d) and 6 (d) within or on grain boundaries where densification occurs by decreasing the pore radius.



(a)1300°C (b)1320 °C

(c) 1340 °C (d) 1360 °C

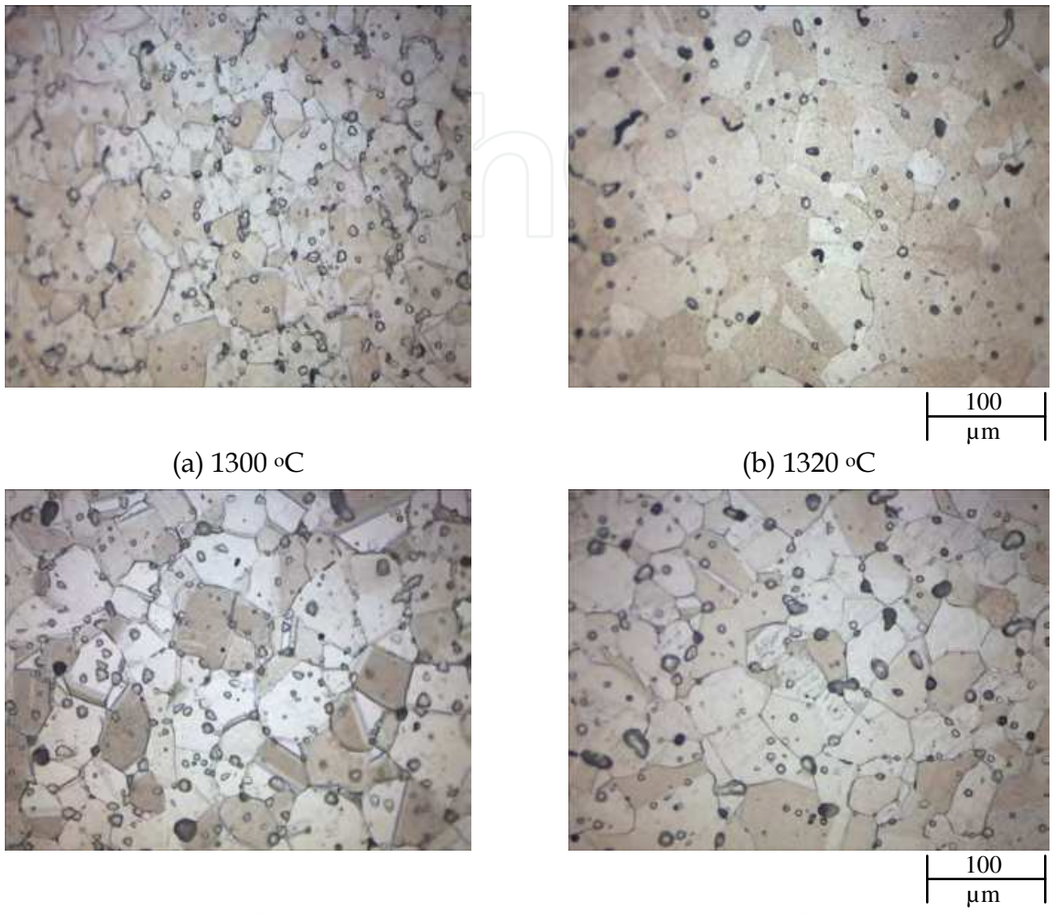
Fig. 5. Optical micrographs of PSPP65-3 specimen sintered at various temperatures. Magnification 500x.

At high densities the pores are mostly associated with the largest grains. Consequently, there is a relation between grain size$G$, pore diameter d_p, and fractional porosity V_p,

$$\frac{G}{d_p} = \frac{K}{RV_p} \tag{1}$$

where R expresses the ratio of attached pores to randomly placed pores and K is a geometric constant. Value of R range from 1.7 to 5.7 for various sintering materials. It should be noted that the degree of boundary-pore contact remains essentially constant during sintering (German, 1996). Indeed, with the prolonged sintering, pore coarsening causes a number of pore size to decrease and that lead to increased grain size. Early in the sintering, the large

pores are immobile and pin the grain boundaries, maintaining a small grain size. Late in sintering there are fewer pores, which are small due to shrinkage and the grains become large. (German, 1996).



(a) 1300 °C (b) 1320 °C

(c) 1340 °C (d) 1360 °C

Fig. 6. Optical micrograph of PSPP65-2 specimen sintered at various temperatures. Magnification 500x.

3.1.2 Mechanical properties

The effect of PS content on tensile strength is shown in Figure 7. It clearly shows that, the specimen PSPP65-4 exhibited tensile strength of greater than 500 MPa for three different sintering temperatures (1320 °C, 1340 °C, 1360 °C). From the standpoint of sintering temperature, an increase in this parameter would increase the sintered strength for all composition tested.

To meet the MPIF Standard 35, the specimens made with 316L SS must have tensile strength of at least 500 MPa. As shown in the Figure 7, all compositions shows a significant linear increment of strength as a result on increasing sintering temperature. High strength greater than 500 MPa was observed in all specimens sintered at 1360 °C, thus complying with the international standard MPIF 35 MIM specimens.

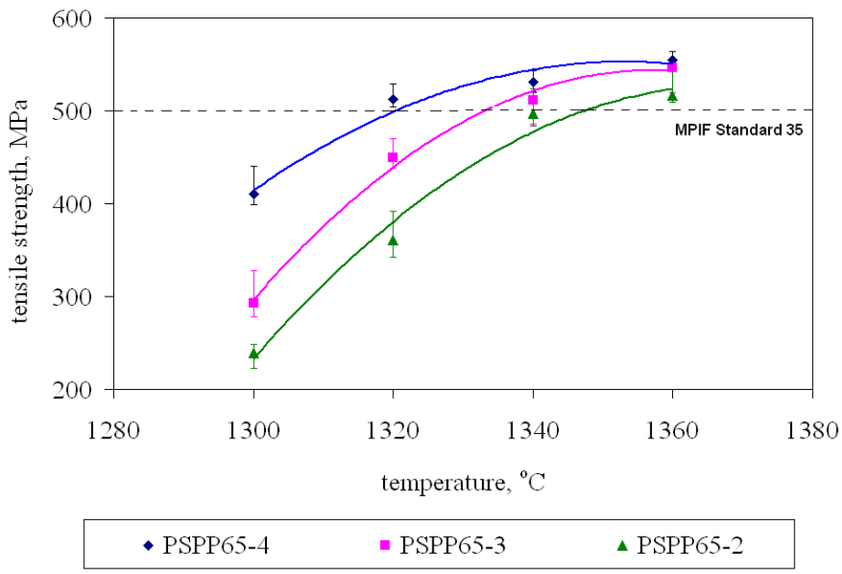


Fig. 7. Effect of the PS content on the sintered strength of specimen sintered at different temperatures.

The sudden increase in strength was obtained when specimens were sintered at 1320 °C especially for specimen of PSPP65-4. These might be due to the changes from intermediate to final stage of sintering that undergoes a transformation to become dense and to be high in strength, with attendant changes in the pore size and shape. Thus, sintering inherently involves substantial shrinkage with elimination of pores that leads to a dramatic increase in strength of specimen. As temperature is increased from 1320 °C to 1360 °C, small deviation changes the strength of all specimens. At this final stage of sintering, coarsening processes consume the surface energy that is responsible for densification, but do not reduce porosity.

The result of hardness of sintered specimens as a function of PS/PP content and sintering temperature is shown in Figure 8. From the results obtained, it can be seen that the hardness of the sintered specimens increases when the sintering temperature increases. The increase in hardness is due to the better densification at higher sintering temperature. It is evident that sintering temperature of 1360 °C gave rise to the highest hardness for all compositions (greater than 200 Hv) that complies with the MPIF Standard 35.

By comparing three properties of sintered density, tensile and hardness, it clearly shows that the higher content of PS has worked successfully in MIM process that complies with the MPIF Standard 35. The sintering temperature of 1360 °C was believed to be sufficient enough to obtain reasonable and acceptable sintered properties.

From the investigation, it clearly showed that the new locally developed binder system using PS as the base material mixed with PP was successful injection moulded with the 316L stainless steel powder. A maximum 70 wt.% of PS was believed to be a promising amount to give sufficient properties that meets the requirement of MPIF Standard 35. This residual carbon which left after debinding, diffuse into the structure of SS 316L powder during sintering and eventually promotes the significant changes of mechanical properties of the sintered specimens.

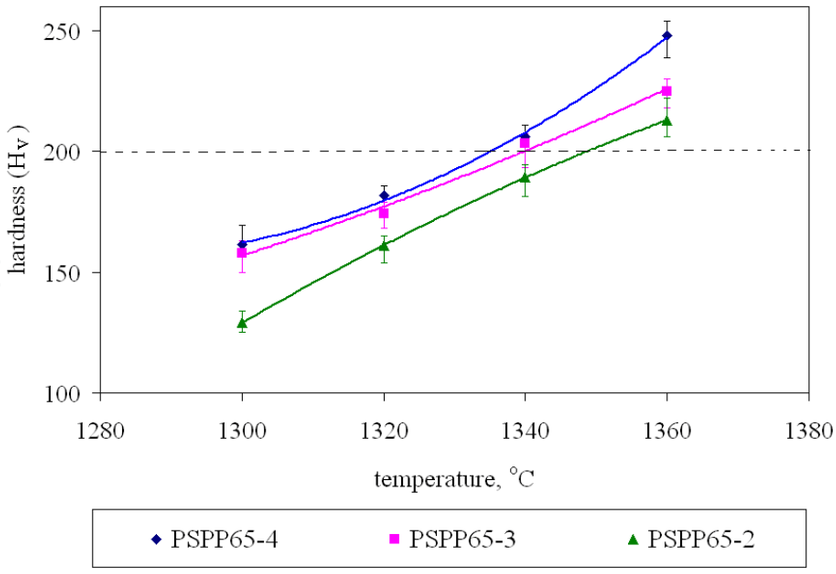


Fig. 8. Effect of the PS content on the hardness (Hv) of specimen sintered at different sintering temperatures.

3.1.3 Sintering study at different heating rate of sintering

The specimen made with 65 vol.% gas atomised 316L SS powder with the composition of binder system PSPP65-4 respectively was sintered at different time, temperature and atmosphere.

Heating rate is important in sintering practice. Too low heating rate at low temperature dissipates driving force and results in nearly no densification, while too high heating rate will result in distortion and warpage. In this study, 3 different heating rates ranging from 5 ^{o}C/min to 15 ^{o}C/min with soaking time of 1 hour were employed. The sintering temperature was kept at 1360 ^{o}C under vacuum atmosphere.

Figure 9 shows the effect of heating rate on the density of the sintered specimens. At the heating rate of 5 ^{o}C/min, the mean density was 7.69 g/cm^{3}, which is approximately 97% of theoretical density. At low heating rate, surface diffusion typically dominates in sintering. This provides bonding without densification, thus resulting in low sintered density of specimen.

From Figure 9, it can be seen that the density increases as the heating rate was increased from 5 ^{o}C/min to 10 ^{o}C/min. However, at heating rate of 15 ^{o}C/min, the density dropped to 7.67 g/cm^{3}, which is approximately 97% of theoretical value. High heating rates induce large thermal stress that accentuates sintering beyond that found in isothermal sintering (German, 1996). At higher temperatures, the densification dominates diffusion resulted in enhance densification without coarsening. Simultaneously, there has been an ability to reduce grain growth while achieving high sintered density.

High density can be achieved as the specimen is sintered at the heating rate of 10 ^{o}C/min. Densification observation of the sintered specimens indicates that the heating rate of 10 ^{o}C/min results in 98 % of theoretical density. Too low heating rate is not preferable for

consideration of economy. From the results obtained, heating rate of 10 °C/min shows to be resulting in the optimum sintered density.

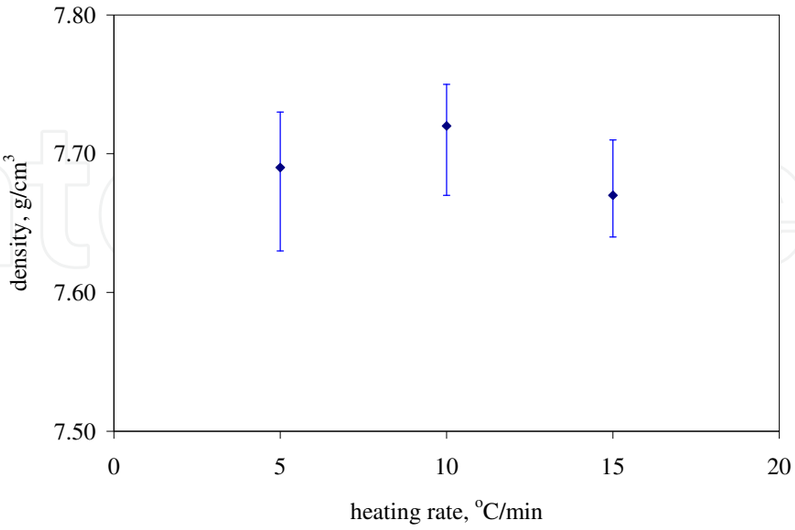


Fig. 9. Density as a function of heating rate.

Figure 10 shows the percentage of porosity at different heating rates. It can be seen that with an increase of heating rate from 5 °C/min to 10 °C/min, the porosity is lower. One effect of slow heating is that pore reducing occurs by surface diffusion. This tends to reduce the driving force for the densification mechanism at the higher temperature. It clearly shows that heating rate of 10 °C/min enabled for the complete diffusion to take place and reducing the number of pores as can be evidenced in Figure 11 (b). However, the numbers of pores increases as the heating rate increase to 15 °C/min. High porosity is due to too fast heating rate and this is probably due to some pores are still remaining prior to isothermal sintering. These pores are isolated and cannot be eliminated due to it being isothermal process. (German, 1996)

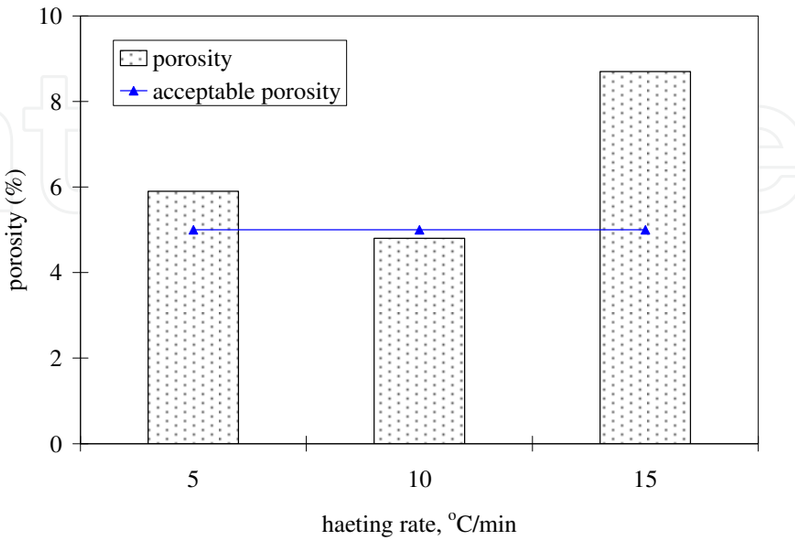
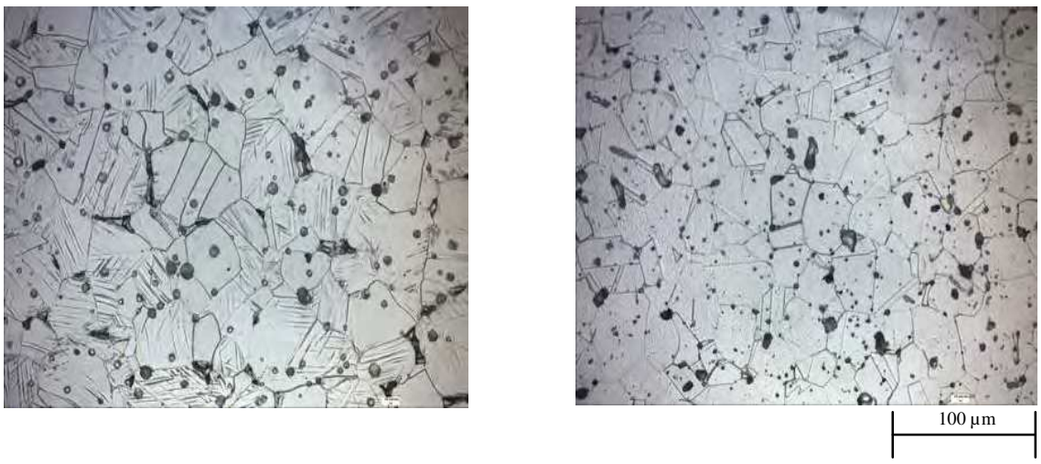


Fig. 10. Porosity as a function of heating rate.

Figure 11 shows the microstructure of the sintered specimens after etching. It can be seen that with an increase in the heating rate, the grain becomes finer. Normally a higher heating rate induces large thermal stresses that accentuate sintering beyond that are found in isothermal sintering (German, 1996). On the other hand, higher heating rate demonstrated an ability to reduce grain growth while achieving high final density. Although the grain boundaries tend to become finer with the heating rate of 15^{o}C/min as shown in Figure 11 (c), the pores within or on the grain boundaries seems to be increasing. High porosity occurs due to too fast heating rate, the metal powder is unable to completely diffuse away. Some pores are still remaining prior to isothermal sintering. These pores are isolated and cannot be eliminated due to isothermal process. These circumstances result in lower sintered density.



(a) 5^{o}C/min (b) 10^{o}C/min

(c)15^{o}C/min

Fig. 11. Microstructure of specimens sintered at different heating rate in vacuum conditions at 1360 ^{o}C. Magnification 500x.

The mechanical properties of the 316L SS samples prepared at various heating rates from 5 ^{o}C/min to 15 ^{o}C/min are compared as shown in Figure 12 and 13. The trends in tensile strength, elongation and hardness for the sintered specimen are similar with density. The tensile strength and elongation increased with the decrease of porosity. At a heating rate of

15 °C/min, the elongation and tensile strength of sintered specimen decreased due to the increasing number of porosity which can be evidenced from the microstructure shown in Figure (c). The greater pore induced the stress concentration that reduced the mechanical properties.

As shown in Figure 12 and 13, heating rates of 10 °C/min shows the highest tensile strength and hardness that can be considered as the optimum schedule for a sintering process. At this heating rate of sintering, near full density was obtained for the specimen tested.

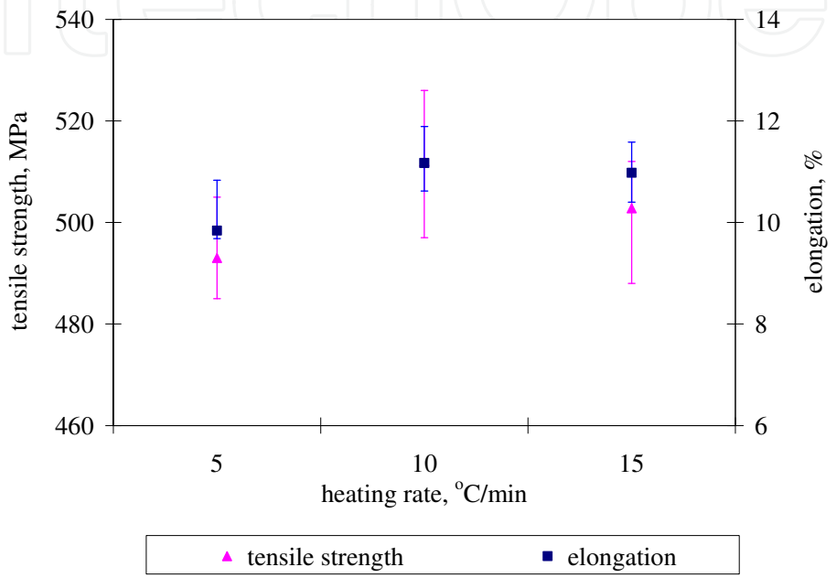


Fig. 12. Tensile strength and elongation as a function of heating rate.

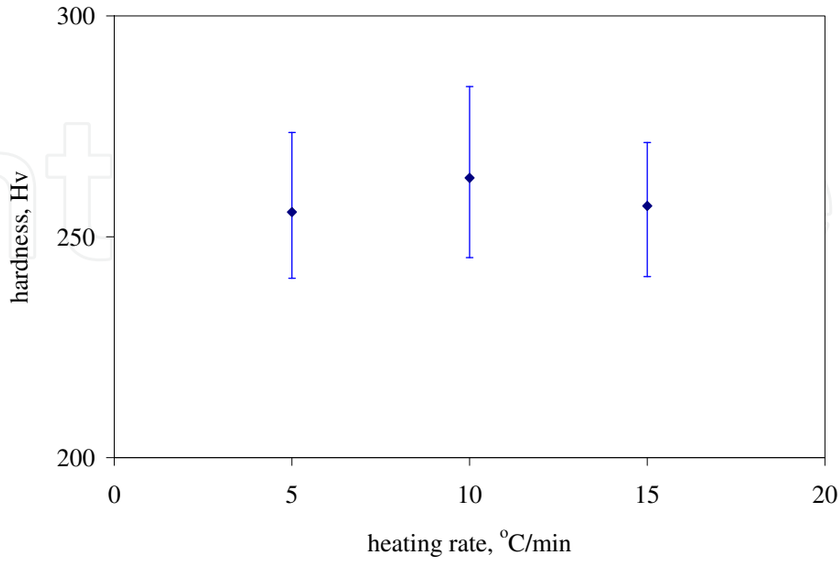


Fig. 13. Hardness as a function of heating rate.

The presence of pores prones to lowering tensile strength, elongation and hardness. This is because the large amount of pores corresponds to a lesser cross sectional area during tensile testing based on the equation of σ=P/A where *P* is pressure or force applied (German, 1996). The strength should decline since pore reduces the load-bearing cross sectional area (*P*). So that, the tensile strength, elongation and hardness are lowered as the porosity of sintered specimen becomes higher. As the consequence, the porosity is considered as an important factor affecting the tensile strength and elongation.

The 316L SS is considered partly as temperature sensitive, thus the optimum heating rate is useful in controlling microstructure evolution since it affects the mechanical properties of sintered specimen. From the results obtained, high physical and mechanical properties of 316L SS were achieved when sintered at 1360 °C with the heating rate of 10 °C/min.

3.1.4 Effect of temperature and atmospheres

Furnace atmosphere does play a critical role during sintering which affects the microstructure, pore size and properties of the sintered specimen. In order to investigate the effect of sintering atmosphere, 3 different atmospheres of vacuum, 95% N_2/5% H_2 and argon were used. Among these atmospheres, sintering in vacuum yields the highest density followed by sintering in 95% N_2/5% H_2 and argon respectively as shown in Figure 14. During heating, the residual gas atmosphere can be trapped in pores that inhibits full densification. As a consequent, high density can be obtained when sintered in vacuum since no gas trapped in the pores. From the result obtained, near full density (97% of theoretical density) was reached at sintering temperature of 1360 °C in the vacuum.

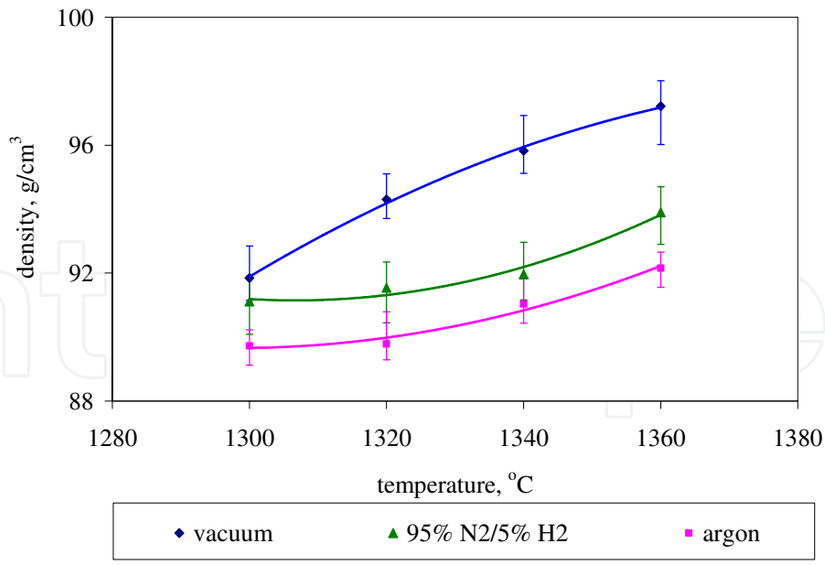


Fig. 14. Densification of 316L SS specimen after sintering in different atmosphere.

There were slight variations in density between sintering in 95% N_2/5% H_2 and in argon as shown in Figure 14. A little variation has been shown for the specimen sintered under 95% N_2/5% H_2 atmosphere in the duration of sintering temperature of 1300 °C to 1340 °C.

However, increasing the sintering temperature to 1360 °C shows a high density achieved which is 90 % of theoretical density.

The result of tensile strength as a function of sintering atmosphere is shown in Figure 15. The trends exhibit by tensile strength and density with temperature are nearly similar, which is increase with increasing sintering temperature. When sintered in vacuum, the maximum ultimate tensile strength of 510.37 MPa was achieved at the temperature of 1360 °C.

The results however show that the tensile strength of specimen sintered under 95% N_2/5% H_2 and argon atmosphere at the temperature in the range of 1300 °C to 1360 °C did not meet the specification of MPIF Standard.

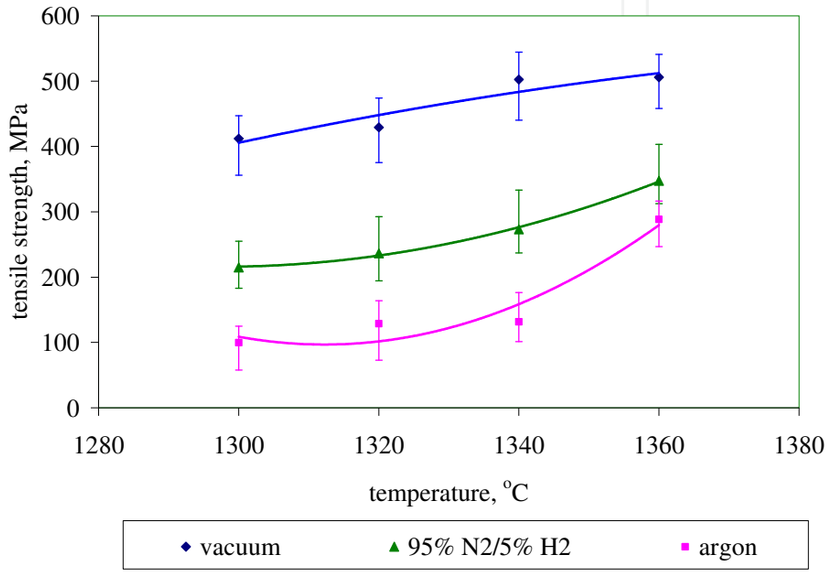


Fig. 15. Tensile strength of 316L SS specimen after sintering in different atmosphere.

The atmosphere (inert) protects surface against contamination during sintering. Additionally, a cleaning function is desired from the atmosphere to remove contamination. In many full-density systems best densification and properties are achieved using vacuum sintering (German, 1996; German and Bose, 1997).

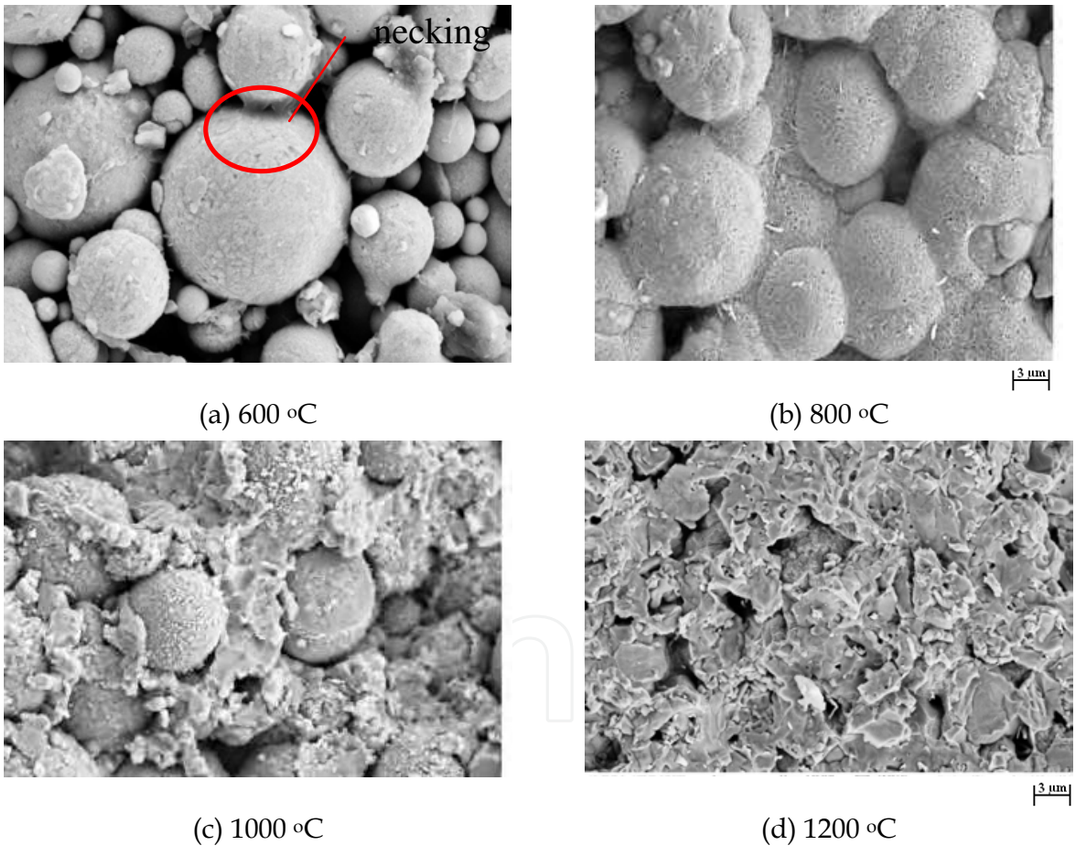
The result obtained shows that the important factors in a sintering cycle are heating rate, temperature and furnace atmosphere. These factors can affect the microstructure, pore size and shape and final density of sintered stainless steel 316L. These in turn influence the mechanical properties of the sintered specimens.

3.1.5 Scanning electron microscopy observation: Microstructure evolution during sintering

The fracture surfaces of the specimen PSPE65-4 shown in Figure 16 reveal clearly the different morphology between the stages of pre-sintering process. The specimens were sintered in a tube atmosphere furnace at different temperatures ranging from 600 °C, to 1200 °C. Figure 16 (a) to (d) demonstrated the progressive microstructural development with increasing temperature during the sintering process.

Sinter bonding is evident as bonds grow at the particle contacts. Figure 16 (a) shows a formation of neck between sintering particles and almost all powder are discretely evident as sintered to 600°C. At the early stage of sintering at 800°C, the powder particles moved to fill the pores by the growth of several necks on each particle as shown in Figure 16 (b). The establishment of interparticles bonds by partial fusion is clearly seen. Increasing the temperature up to 1000°C extends the fusion bonding further with a substantial reduction in porosity. The particles take many paths to form the bonds. The original shape of the powders can still be discerned, although the particles have been fused together.

As the bonds become larger, they impinge on each other and form a network of pores as shown in Figure 16 (d). These pores are termed open pores that are accessible from the compact surface, so the sintering atmosphere can move in or out of the pores during sintering. The open pores are attributed to a lower elongation of sintered specimen corresponding to an intermediate stage of sintering.



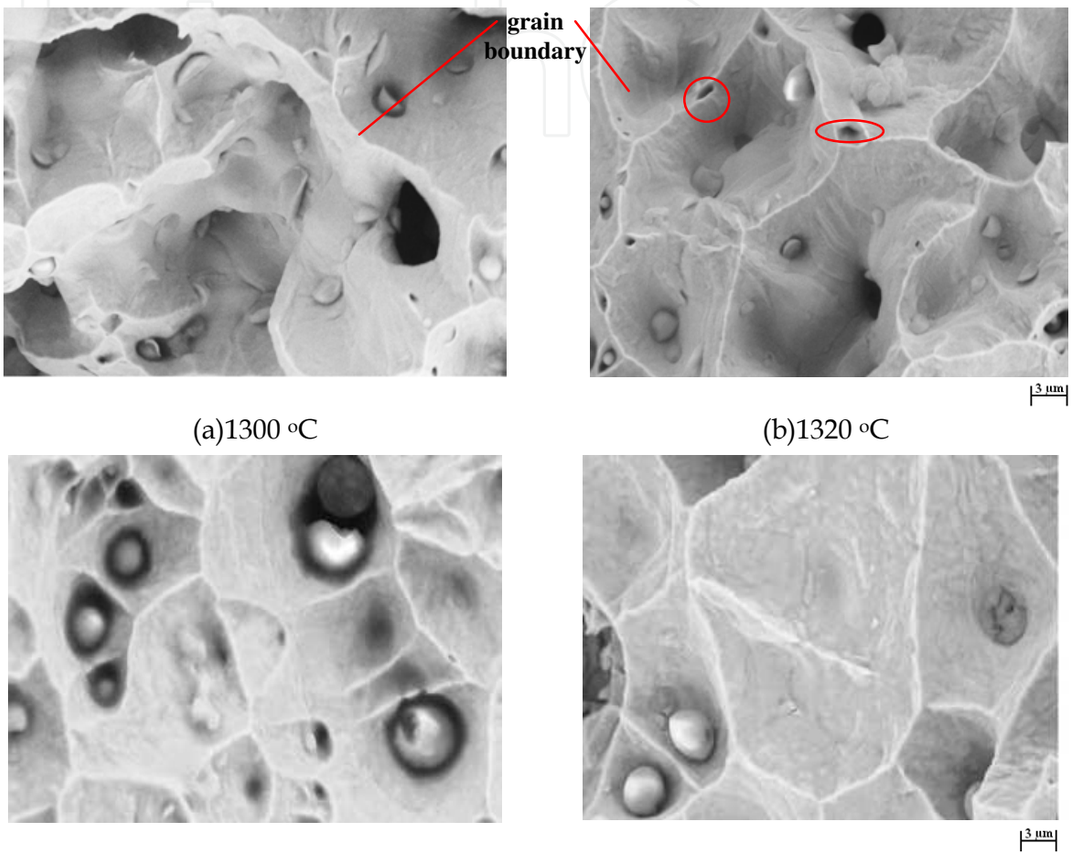
(a) 600 °C (b) 800 °C

(c) 1000 °C (d) 1200 °C

Fig. 16. Scanning electron micrograph of fracture surface of specimen after presintering at different temperatures.

During sintering, the initially loose powder compact undergoes a transformation to become a dense, polycrystalline structure with physical and mechanical properties similar to engineering materials. The final stage of sintering has a few pores sitting on grain boundaries.

Figure 17 depicts the SEM micrographs of vacuum sintered SS 316L specimens (PSPP65-4) at different temperatures ranging from 1300 °C to 1380 °C. At 1300 °C, it clearly shows that the powder boundaries were replaced by grain boundaries as shown in Figure 17 (a). As the temperature was increased, the microstructure began to coarsen that considerable reduces surface area, increases grain size and compact strengthening with attendant changes in the pore size and shape.



(a)1300 °C (b)1320 °C

(c) 1340 °C (d) 1360 °C

Fig. 17. Scanning electron micrograph showing the fracture surface of 316L stainless steel specimen sintered at various temperatures.

Sample sintered at 1320 °C shows spherodising and shrinking of pores , which are not connected to the compact surface (Figure 17 (b)). These pores are termed closed pores. The pore located on grain boundaries as shown in Figure 17 (a) disappeared as temperature increased, but pores disconnected from grain boundaries remain stable as shown in Figure 17 (c) and (d). The typical ductile fracture mechanisms is evidenced by dimples in the final stage of sintering as can be seen in Figures 17(c) and (d). A few isolated pores (closed pores) can also be observed in the Figures 17 (c) and (d) suggesting that closed pores play little part in the fracture. These closed pores are sealed and inaccessible via the sintering atmosphere.

In many literatures, sintering of stainless steel was carried out in the range of 1300 °C and 1380 °C (White and German, 1995; Cai and Geman, 1995; Loh et al., 1996; Afian, 1999). However, in this study, as the sintering temperature rose up to 1380 °C, separation has been noticed.

Besides that, sample experienced swelling defect and deteriorates. The specimen was to swell and changed the shape required. Figure 18 shows the fracture surface of specimen sintered at 1380 °C. At this stage, the sintering is faster as temperature approaches the melting point because of the increased number of moving atoms resulted in the atoms landing at the bond between particles where it helps annihilate surface area and surface energy (German, 1996).Figure 18 clearly shows the greater size of pores indicating that more energy had been activated. These large pores are unable to remain attached to moving grain boundaries and become stranded at the grain interior. The grain boundary tends to break away from the pores. The growth of the pores could cause a decrease in density during prolonged final stage sintering. As 316L SS has a melting temperature of 1441°C , it is preferable to sinter the specimen ranging between 1300 °C and 1360 °C.

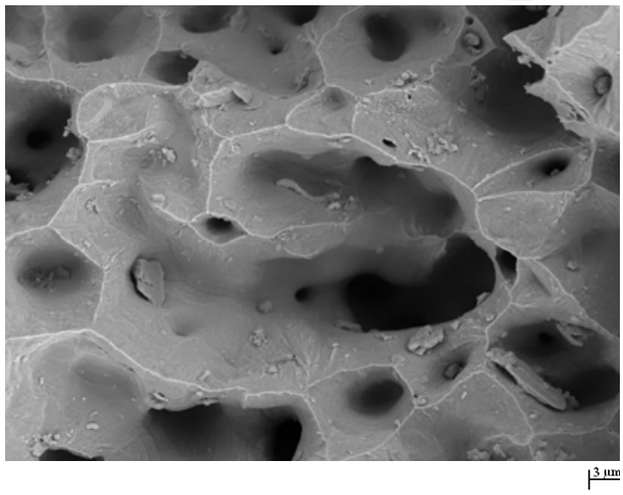


Fig. 18. Scanning electron micrograph of fracture surface of specimen sintered at 1380 °C.

There are many fine particles that appeared in the centre of a grain boundary. These particles have a dimension of approximately 3 µm. As shown in Figure 19, the energy dispersive spectroscopy (EDS) result shows that this is the particles which is not diffused and appeared exclusively. Table 3 shows the elements found in the particles.

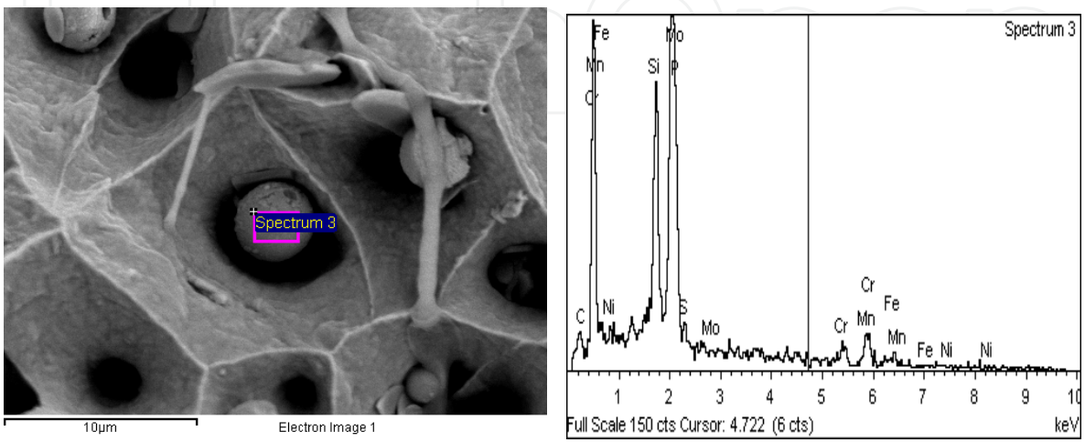


Fig. 19. Energy dispersive spectroscopy of sintered specimen.

Element	Weight %
C K	4.27
Si K	13.68
P K	5.74
S K	3.62
Cr L	61.39
Mn L	0.00
Fe L	11.30
Ni L	0.00
Mo L	0.00
Total	100%

Table 3. EDS results showing the elements present in the fine particles.

4. Conclusion

The new developed binder systems, palm stearin can be used as a binder system combined with polypropylene in the metal injection moulding process. The maximum metal powder loading in the powder/binder mixture for successful injection moulding was 65 vol.% for gas-atomised 316L stainless steel.

The sintering process of injection moulded 316L stainless steel specimen is clearly influenced by sintering temperature. With a high sintering temperature, the density shrinkage, tensile strength and the hardness of the sintered specimens increase due to the pore shrinkage. The closure of the pores enhanced the mechanical properties of the sintered samples. From this study, it can be concluded that the best sintering temperature for the 316L stainless steel powder using palm based binder is 1360°C which result in good properties for the sintered parts, and comply with the requirement for MPIF Standard 35 for Metal Injection Moulded Parts.

5. Acknowledgment

The authors would like to thank MOSTI for financial support under ScienceFund grant No. 03-03-02-SF0040, 03-03-03-SF0124 and TechnoFund 1208D168.

6. References

Berginc,B., Kampus, Z and Sustarsic, B. (2007). Influence of feedstock charateristics and process parameters on peroperties on MIM parts made of 316L stainless steel, *Powder Metallurgy*, 50 , 172-183

German, R. M. & Donal, K. (1993). Evaluation of injection moulded 17-4 PH stainless steel using water atomized powder. *The International Journal of Powder Metallurgy*, 29(1), 47-61

German, R.M, (1996), *Sintering Theory and Practice*, John Wiley and Sons, Inc, New York

German, R.M. & Hens, K.F. (1992). Identification of the effect of key powder characteristics in PIM. *Proc. of Powder Injection Moulding Symposium*, MPIF, Princeton, NJ, 1-16.

German, R.M. (1993). Technological barriers & opportunities in powder injection moulding. *Powder Metallurgy International*, 25(4), 165-168.

German, R.M. and Bose, (1997) *A. Injection Moulding of metal and Ceramis*, MPIF, Princeton , NJ.

German, R.M., (1990), *Powder Injection Moulding*, Princeton , New York.

Iriany, (2002), PhD Thesis, Universiti Kebangsaan Malaysia, Malaysia

Istikamah, S., (2010), PhD Thesis, Universiti Teknologi Mara, Malaysia

Li, Y., Li, L. and Khalil, K.A. (2007). Effect of Powder Loading on Metal Injection Moulding Stainless Steels, *Journal of Materials Processing Technology*, 183, 432-439

Omar, M.A., (2006) Metal injection Moulding- An Advanced Processing Technology", *Journals of Industrial Technology*, 15 (1) , 11-22

Omar, M.A., and Subuki, I., (2007) Rapid Debinding of 316L Stainless Steel Injection Moulded Using Palm Based Biopolymer Binder, Proceedings of 3rd Cooloquium on Postgraduate Research on Materials, Minerals and Polymers 2007, Vistana Hotel, Penang

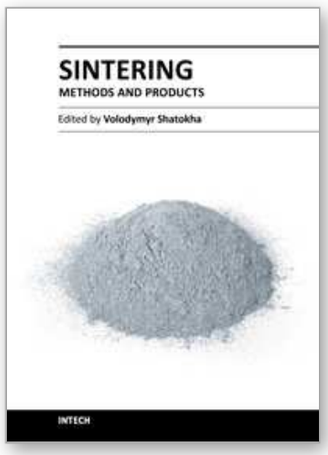
Omar, M.A.,, .Subuki, I and Ismail, M.H., (2006) . Observation of Microstructural Changes During Solvent Extraction and Polymer Burnout Process of MIM Compact", Proceedings of 5th International Materials Technology Conference and Exhibition 2006 (IMTCE 2006), July, 2006, Kuala Lumpur

Omar**,**M.A**.,** Davies, H.A., Messer, P.F. and Ellis,B. (2001). The Influence of PMMA Content on the Properties of 316L Stainless Steel MIM Compact, *Journal of Materials Processing Technology*, 113 :477-481.

Omar**,**M.A**.,** Mohamad, M., Sidik, M.I. and Mustapha, M. (2002). A PEG-based Binder System for Metal Injection Moulding, *Solid State Science and Technology*, **10**, No. 1& 2 : 359-364

Zhang,H and German, R.M. (1991). Structural development During Sintering on Injection Moulded Fe-2Ni Steel, *Advances in Powder Metallurgy*, 2,:181-194

IntechOpen



Sintering - Methods and Products

Edited by Dr. Volodymyr Shatokha

ISBN 978-953-51-0371-4
Hard cover, 316 pages
Publisher InTech
Published online 23, March, 2012
Published in print edition March, 2012

This book is addressed to a large and multidisciplinary audience of researchers and students dealing with or interested in sintering. Though commonly known as a method for production of objects from fines or powders, sintering is a very complex physicochemical phenomenon. It is complex because it involves a number of phenomena exhibiting themselves in various heterogeneous material systems, in a wide temperature range, and in different physical states. It is multidisciplinary research area because understanding of sintering requires a broad knowledge - from solid state physics and fluid dynamics to thermodynamics and kinetics of chemical reactions. Finally, sintering is not only a phenomenon. As a material processing method, sintering embraces the wide group of technologies used to obtain such different products as for example iron ore agglomerate and luminescent powders. As a matter of fact, this publication is a rare opportunity to connect the researchers involved in different domains of sintering in a single book.

How to reference

In order to correctly reference this scholarly work, feel free to copy and paste the following:

Mohd Afian Omar and Istikamah Subuki (2012). Sintering Characteristics of Injection Moulded 316L Component Using Palm-Based Biopolymer Binder, Sintering - Methods and Products, Dr. Volodymyr Shatokha (Ed.), ISBN: 978-953-51-0371-4, InTech, Available from: http://www.intechopen.com/books/sintering-methods-and-products/sintering-characteristics-of-injection-moulded-components-using-palm-based-biopolymer-binder-

INTECH
open science | open minds

InTech Europe
University Campus STeP Ri
Slavka Krautzeka 83/A
51000 Rijeka, Croatia
Phone: +385 (51) 770 447
Fax: +385 (51) 686 166
www.intechopen.com

InTech China
Unit 405, Office Block, Hotel Equatorial Shanghai
No.65, Yan An Road (West), Shanghai, 200040, China
中国上海市延安西路65号上海国际贵都大饭店办公楼405单元
Phone: +86-21-62489820
Fax: +86-21-62489821

© 2012 The Author(s). Licensee IntechOpen. This is an open access article distributed under the terms of the Creative Commons Attribution 3.0 License, which permits unrestricted use, distribution, and reproduction in any medium, provided the original work is properly cited.

IntechOpen

IntechOpen